Dynamical Heterogeneity and Jamming in Glass-Forming Liquids[†]

Naida Lačević[‡,§] and Sharon C. Glotzer*[,‡,‖]

Departments of Chemical Engineering and of Materials Science and Engineering,
University of Michigan, Ann Arbor, Michigan 48109

Received: May 27, 2004; In Final Form: October 25, 2004

The relationship between spatially heterogeneous dynamics (SHD) and jamming is studied in a glass-forming binary Lennard-Jones system via molecular dynamics simulations. It has been suggested [*Phys. Rev. Lett.* **2001,** *86,* 111][1] that the probability distribution of interparticle forces $P(F)$ develops a peak at the glass transition temperature T_g and that the large force inhomogeneities, responsible for structural arrest in granular materials, are related to dynamical heterogeneities in supercooled liquids that form glasses. It has been further suggested that "force chains" present in granular materials may exist in supercooled liquids and may provide an order parameter for the glass transition. Our goal is to investigate the extent to which the forces experienced by particles in a glass-forming liquid are related to SHD and compare these forces to those observed in granular materials and other glass-forming systems. Our results are summarized as follows. We calculate $P(F)$ for positive (repulsive) instantaneous forces and find no peak in $P(F)$ at any temperature in our system, even below T_g. We also find that particles that have been localized for a long time are less likely to experience high relative force and that mobile particles experience higher relative forces at shorter time scales, indicating a correlation between pairwise forces and particle mobility. We construct force chains based on the magnitude of pairwise positive instantaneous forces. We find that force chains constructed in this manner are composed of both localized and mobile particles; therefore there is no one-to-one correspondence between force chains as defined here and locally mobile or immobile regions of the liquid. We also find that force chains do not play the same role as force chains in granular materials but may indicate a difference in the evolution of the local environment of particles with different mobility. We also discuss a possible relationship between force chains found here and the development of stringlike motion found in this and other glass-forming liquids [*Phys. Rev. Lett.* **1998,** *80,* 2338; *J. Chem. Phys.* **2004,** *120,* 4415].[2,3]

I. Introduction

Attempts are underway in the statistical mechanics community to unify concepts regarding supercooled liquids and granular materials, two very different classes of systems that display similar behavior in many respects. Systems near their glass transition, colloidal suspensions at large pressures or densities, foams under shear, granular materials under "tapping" or shearing, and other systems such as bubbles and droplets "jam" under certain circumstances. Jamming is also seen in polymer crazes.[4] Jamming is a process in which systems appear "stuck" in phase space because their particles come in close contact with each other, resulting in structural arrest. This process sketches what happens with supercooled liquids at the glass transition temperature T_g, where jamming is controlled by the temperature or density. In colloidal suspensions under high pressure or at high density, particles also get "stuck", and the suspension acts as an amorphous solid.[5] Foams or emulsions flow under high shear rate, but at low shear they stop flowing and appear to be solids as well.[6] Extensive reviews of granular materials can be found in refs 7–9. Among many experiments that deal with the behavior of granular materials under external perturbation, refs 10–12 indicate that the response of granular

materials upon isolated tapping or continuous vibration is similar to the response of supercooled liquids near T_g. In these experiments, the density fluctuations of a granular material subject to shaking were investigated by reducing the shaking frequency until the granular material reached a "jammed" configuration.

What are the similarities and differences between glass-forming liquids and granular materials? First we note some of the properties of granular materials. Unlike glass-forming liquids, granular materials consist of a large number of particles that are individually solid (grains). The grain-grain interactions are classical because the size of the grains is much larger than the de Broglie wavelength. The grains exert forces only when they are in contact and may be surrounded by a fluid (typically air) or a vacuum. The collisions between grains are in general inelastic. The main difference between liquids and granular materials, aside from the obvious difference of length and time scale, is the concomitant difference in energy scales. In granular materials, thermal energies $k_b T$ are insignificant compared to the energy it takes to move a single particle. Thermal energy in the liquid allows it to explore different states, whereas the low relative magnitude of thermal energy in a granular material does not allow it to sample other configurations unless energy is added to the system. This means that granular materials can stay in a metastable state indefinitely.

A schematic "jamming" phase diagram was proposed in ref 13 to unite the concepts of jamming in many different systems. According to the diagram, jamming in supercooled liquids occurs at low temperature T and high pressure P. Such a unified

---

picture prompts several questions, such as whether the dynamics of different systems approaching the jammed state are similar. The jamming phase diagram suggests that the glass and jammed states may be related. However, the details of this relationship are not yet fully understood. For instance, a commonly measured quantity in granular materials is the probability distribution of normal forces $P(F)$. $P(F)$ develops a peak near the jamming transition in granular materials that is well established in experiments and computer simulations. It has been suggested that a similar peak in $P(F)$ measured in supercooled liquids signifies the onset of solidity, and consequently is a signature of the glass transition. The obvious supposition is: if the link between jamming and the glass transition exists, then the mechanism for slowing down of dynamics in supercooled liquids may be related to macroscopic structural arrest in granular materials. A peak in $P(F)$ at and below T_g would provide a link in this regard. Such a peak was reported in 2D simulations of several glass-forming liquids.[1] We test the generality of this result in the present work.

As shown in many experiments and computer simulations of granular materials,[14-18] large force inhomogeneities are responsible for structural arrest under shear. If the shear rate is sufficiently low, the granular material will be structurally "arrested" or jammed. Jamming in granular materials occurs because the particles form force chains along the direction in which the stress is applied.[19] Recently, Kustanovich et al.[20] investigated the organization of atomic bond tensions and the relationship with force chains in several models of glasses. They observed force chains in 2D and 3D glasses only at zero temperature, and concluded that the balance of forces on each atom is a necessary condition for force chain formation. This leads us to pose the following question: Do force chains exist in supercooled liquids, and if so, are they responsible for the slowing down of dynamics, and related to other prominent features of supercooled liquids?

A salient feature of glass-forming liquids whose origin is still not understood is the spatially heterogeneous nature of their dynamics. In particular, the nonexponential character of the relaxation of density correlation functions and decoupling of the transport coefficients can be rationalized with the existence of *spatially heterogeneous dynamics* (SHD) or "dynamical heterogeneity". We refer to a system as dynamically heterogeneous if it is possible to select a dynamically distinguishable subset of particles by experiment or computer simulation.[21] Simulations[22-28] and experiments[29-44] have demonstrated the cooperative and spatially heterogeneous nature of the liquid dynamics (for reviews of the experimental evidence for spatially heterogeneous dynamics, see, e.g., refs 45-47).

In refs 2, 28, and 48-53, several approaches—including calculation of a displacement-displacement correlation function, identification of clusters of mobile particles, and calculation of a four-point time-dependent density correlation function—predicted and demonstrated the importance of spatially heterogeneous dynamics in supercooled liquids using a rigorous statistical mechanical analysis. In particular, using the four-point time-dependent density correlation function formalism, we found dynamical correlation lengths of regions of localized and delocalized particles that suggest a picture of fluctuating domains of temporarily localized and delocalized particles, as suggested by Stillinger and Hodgedon.[54] It has recently been demonstrated in two simulated liquids[55] that these fluctuating domains are dynamically facilitated, as predicted by Garrahan and Chandler.[56] Many specific predictions made possible through such analyses have now been confirmed in experiments on colloidal

suspensions.[40,41,57] The tools from these analyses are thus available to investigate the connection between jamming in granular materials and SHD in supercooled liquids. In this work, we will use the four-point time-dependent density correlation function formalism to test this connection.

Here we analyze the instantaneous, positive (repulsive) forces experienced by particles in a glass-forming liquid in analogy to contact (normal) forces experienced by particles in granular materials. We investigate $P(F)$, and attempt to ascertain a relationship between the forces and spatially heterogeneous dynamics. The paper is organized as follows. In section 2, we describe the model and method used to produce our results. In section 3, we give a brief description of SHD and the theoretical framework used to describe SHD in this paper. In section 4, we measure the instantaneous positive forces between all particle pairs in our glass-forming liquid, calculate the force distribution $P(F)$, the average force and corresponding standard deviation for every T simulated. In this section, we compare $P(F)$ to force distributions found in granular and other glassy systems. Sections 5-7 focus on the relationship between instantaneous positive forces and particle mobility. In section 5, we define "paths" of highest, average, and lowest positive forces, which we call "force chains", and investigate the temperature dependence of their average mass, average number, and mass distribution. In section 6, we divide the set of instantaneous positive pair forces for each configuration into subsets of highest, average and lowest forces at each T. Using our definition of localized and replaced particles (defined in section 3), we find the fractions of these particles in each subset of instantaneous pair forces. In section 7, we investigate the fractions of localized and replaced particles in "force chains". We conclude with a discussion of our results in section 8.

II. Model and Method

The simulation method we use to generate data for our analyses is molecular dynamics (MD). This is a widely used method in the investigation of supercooled liquids and glasses that provides static and dynamic properties for a collection of particles described by classical force fields. To perform our simulations we use LAMMPS,[58] a parallel MD code developed by Plimpton. We study a 50/50 binary mixture of particle types "A" and "B" that interact via the Lennard-Jones potential

$$V_{\alpha\beta}(r) = 4\epsilon_{\alpha\beta}\left[\left(\frac{\sigma_{\alpha\beta}}{r}\right)^{12} - \left(\frac{\sigma_{\alpha\beta}}{r}\right)^{6}\right] \tag{1}$$

This system has been extensively studied by Wahnström,[59] Schrøder,[60] and our group.[61,62] Following previous work, we use length parameters $\sigma_{AA} = 1$, $\sigma_{BB} = 5/6$, and $\sigma_{AB} = (\sigma_{AA} + \sigma_{BB})/2$, and energy parameters $\epsilon_{AA} = \epsilon_{BB} = \epsilon_{AB} = 1$. The masses of the particles are chosen to be $m_A = 2$ and $m_B = 1$. We shift the potential in the usual way and truncate it so it vanishes at $r = 2.5\sigma_{AB}$.

We simulate a system of $N = 8000$ particles using periodic boundary conditions in a cubic box of length $L = 18.334$ in units of σ_{AA}, which yields a density of $\rho = N/L^3 = 1.296$ for all state points. We report time in units of $\tau = (m_B\sigma_{AA}^2/48\epsilon_{AA})^{1/2}$, length in units of σ_{AA}, and temperature, T, in units of ϵ_{AA}/k_B, where k_B is Boltzmann's constant. We simulate state points in the *NVE* ensemble at temperatures ranging from $T = 2.0$ to $T = 0.001$, following a path similar to that followed in refs 60-63. Additionally, we simulate a series of state points in the *NPT* ensemble for temperatures ranging from 0.1 to 0.6 at zero average pressure. Simulation details can be found in refs 53

Heterogeneity and Jamming in Glass-Forming Liquids

J. Phys. Chem. B, Vol. 108, No. 51, 2004 **19625**

TABLE 1: Average Temperature $\langle T \rangle$ and Relaxation Time τ_α for the System Simulated in the NVE Ensemble

$\langle T \rangle$	τ_α
0.588 ± 0.001	3500 ± 100
0.598 ± 0.002	1900 ± 100
0.615 ± 0.001	880 ± 50
0.637 ± 0.001	370 ± 50
0.660 ± 0.001	240 ± 30
0.689 ± 0.001	150 ± 30
0.944 ± 0.001	16 ± 5
2.004 ± 0.001	4 ± 1

and 64. We estimate the mode coupling temperature $T_{MCT} = 0.57 \pm 0.01$, (the glass transition temperature T_g is typically in the range $0.6T_{MCT} < T_g < 0.9T_{MCT}$[65]) and the Kauzmann temperature T_0, which can be considered a lower bound for the glass transition temperature T_g, is $T_0 = 0.48 \pm 0.02$. These quantities are found by calculating the structural relaxation time τ_α in systems simulated above T_{MCT} by fitting the secondary relaxation of the coherent intermediate scattering function $F(q_0,t)$, evaluated at wavevector q_0 corresponding to the largest peak in the static structure factor, to a stretched exponential function $F(t) = A \exp(-(t/\tau_\alpha)^\beta)$. Table 1 summarizes the T dependence of τ_α for the simulations in the *NVE* ensemble.

III. Quantities Used To Measure Spatially Heterogeneous Dynamics

The quantities relevant to SHD that we use here were calculated in ref 53 using a theoretical framework based on a four-point time-dependent, density correlation function $g_4(r,t)$. Here, we give definitions of these quantities that will be used in later sections of the paper. The quantity $g_4(r,t)$ is related to an order parameter $Q(t)$ corresponding to the number of "overlapping" particles in a time window t, where the term "overlap" is used to denote a particle that was either localized or replaced in a time t. Mathematically, $Q(t)$ is defined as

$$Q(t) = \int d\mathbf{r}_1 d\mathbf{r}_2 \rho(\mathbf{r}_1,0)\, \rho(\mathbf{r}_2,t)\, w(|\mathbf{r}_1-\mathbf{r}_2|) =$$
$$\sum_{i=1}^{N}\sum_{j=1}^{N} w(|\mathbf{r}_i(0)-\mathbf{r}_j(t)|) \quad (2)$$

where $w(|\mathbf{r}_1-\mathbf{r}_2|)$ is unity for $|\mathbf{r}_1 - \mathbf{r}_2| \leq a$ and zero otherwise. As in previous work, we take $a = 0.3$; a discussion of the sensitivity of quantities such as $Q(t)$ to the choice of a is given in ref 53. The reason for introducing an "overlap" function w is to eliminate the vibrational motion of the particles, which is known to be only weakly correlated at best (for more details, see, e.g., ref 53). In refs 53 and 61, we showed that $Q(t)$ can be decomposed into self and distinct components,

$$Q(t) = Q_S(t) + Q_D(t) =$$
$$\sum_{i=1}^{N} w(|\mathbf{r}_i(t)-\mathbf{r}_i(0)|) + \sum_{i=1}^{N}\sum_{i\neq j}^{N} w(|\mathbf{r}_i(0)-\mathbf{r}_j(t)|) \quad (3)$$

The self part, $Q_S(t)$, measures the number of particles that move less than a distance a in a time interval t; we call these "localized" particles. The distinct part, $Q_D(t)$ measures the number of particles replaced within a radius a by another particle in time t; we call these "replaced" particles.

We also consider "delocalized" particles, that is, particles that in a time t moved more than a distance a from their original location. As was pointed out in ref 61, substituting $1 - w$ for w in eq 2 gives the delocalized order parameter $Q_{DL}(t) = N - Q_S(t)$.
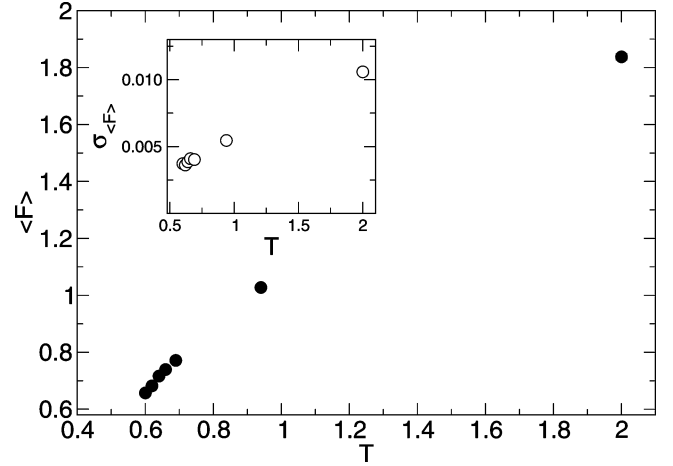

Figure 1. T dependence of the average force $\langle F \rangle$. The inset shows the T dependence of the standard deviation $\sigma_{\langle F \rangle}$. The error bars on $\langle F \rangle$ and $\sigma_{\langle F \rangle}$ are smaller than the symbol size.

The fluctuations, $\chi_4(t)$, in $Q(t)$ may be defined as

$$\chi_4(t) = \frac{\beta V}{N^2}[\langle Q(t)^2 \rangle - \langle Q(t) \rangle^2] \quad (4)$$

Following the scheme of decomposing $Q(t)$, $\chi_4(t)$ can be decomposed into self $\chi_{SS}(t)$, distinct $\chi_{DD}(t)$, and cross $\chi_{SD}(t)$ terms. $\chi_{SS}(t) = \chi_{DL}(t)$ is the susceptibility arising from fluctuations in the number of localized particles, $\chi_{DD}(t)$ is the susceptibility arising from fluctuations in the number of particles that are replaced by a neighboring particle, $\chi_{SD}(t)$ represents cross fluctuations between the number of localized and replaced particles, and χ_{DL} is the susceptibility arising from fluctuations in the number of delocalized particles.

$\chi_4(t)$ (and its terms) measures the correlated motion between pairs of particles, calculated equivalently from fluctuations in the number of overlaps or from the four-point correlation function itself.[53] As shown in ref 53, the behavior of $\chi_4(t)$ demonstrates that correlations are time dependent, with a maximum at a time t_4^{max}. The characteristic times t_4^{max} and τ_α (defined in the previous section) have similar T dependence, and the correlations measured by $\chi_4(t)$ are most pronounced in the α-relaxation regime.

IV. Instantaneous Positive Force Distribution Function $P(F)$ and Average Force

Because we are studying a dense liquid described by a relatively short-range pair potential, at any instant in time each particle experiences a force due to the presence of neighboring particles. Following ref 1, we calculate the average force $\langle F \rangle$ between every pair of neighboring particles at a given instant of time. In analogy with granular materials that are typically modeled as hard spheres with positive contact forces, we consider only positive forces, i.e., forces between particles that are first nearest neighbors at the high densities we study.

In Figure 1 we show $\langle F \rangle$ vs T calculated from at least $N_{conf} = 1000$ independent *NVE* configurations at each T. We see that both $\langle F \rangle$ and the standard deviation

$$\sigma_{\langle F \rangle} = \left(\frac{1}{N_{conf}(N_{conf} - 1)} \sum_c (\langle F \rangle_c - \langle F \rangle)^2 \right)^{1/2}$$

where $\langle F \rangle_c$ is the average force for a particular configuration (c), decrease with decreasing T. [We also find that the standard
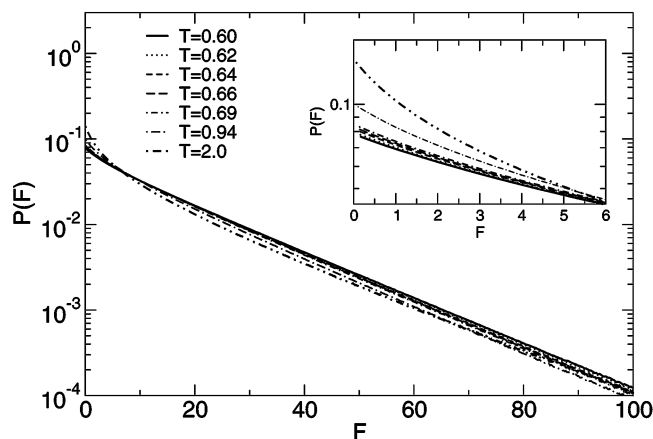
Figure 2. *T* dependence of $P(F)$ vs F. The inset shows the behavior of $P(F)$ for small positive forces.

Figure 3. *T* dependence of the force distribution $P(F/\langle F \rangle_c)$ vs $F/\langle F \rangle_c$. Forces that are much larger than $\langle F \rangle$ decay exponentially. The curvature of $P(F/\langle F \rangle_c)$ around $F/\langle F \rangle_c = 1$ does not change sign, but its value decreases as *T* decreases. The inset shows a close-up of $P(F)/\langle F \rangle_c$ for forces near $\langle F \rangle_c$.

deviation $\sigma_{\langle F \rangle}$ calculated *within* each configuration has the same temperature dependence (not shown).] A decrease is expected because the average pressure (see Table 1 in ref 53) in our constant volume NVE simulation decreases as *T* decreases. Large $\sigma_{\langle F \rangle}$ at higher *T* is also expected because of the larger fluctuations in pressure at higher temperatures.

$\langle F \rangle$ is calculated in the following manner. First, the average force of a particular configuration c is found from $\langle F \rangle_c = (\sum_{ij} F_{ij})/N_{ij}$, where N_{ij} is the number of pairs *i* and *j* for which the force is nonzero, and particles *i* and *j* belong to that particular configuration. An ensemble average force $\langle F \rangle$ is calculated as an equally weighted average over all $\langle F \rangle_c$. This can be an important point when there are large force fluctuations that result in substantially different numbers of positive forces for different configurations. We have, however, checked an alternative method to calculate the average force by calculating the average force from all particle pairs, making no distinction between configurations, and obtained the same answer, indicating that the system is self-averaging. In ref 66 the authors showed that the presence of non-self-averaging alters the force distribution function $P(F)$, which we now consider.

In foams and granular materials, $P(F)$ is measured as a distribution of interparticle normal forces.[67,68] In our system, there is no strict definition of point contact between Lennard-Jones (LJ) particles, and therefore the normal force between particles in not well-defined. We define two LJ particles to be in contact if they interact with a positive (repulsive) force, as was done in ref 1. Commonly, granular materials are modeled as systems of particles with only repulsive interactions when grains are in contact. Therefore, we investigate $P(F)$ only for the subset of positive (repulsive) *F*.

Figure 2 shows the *T* dependence of the force distribution function $P(F)$, calculated as a normalized histogram of all instantaneous positive forces between particle pairs. The behavior of $P(F)$ is similar to the one observed in ref 1 for their LJ system above T_g. We observe an exponential tail at high forces and an increase in the curvature of $P(F)$ at small forces as *T* decreases. An explanation of the origin of the long exponential tail in $P(F)$ was proposed in ref 1 and is related to the fact that large *F* behavior can be obtained from the small *r* behavior of $g(r) \approx y(r) \exp[-V(r)/k_b T]$ and $P(F) \, dF \propto g(r) \, dr$. The exponential tail in the force distribution of granular materials was suggested in the *q*-model in ref 69 to be a consequence of a force randomization throughout the packing. This randomization has an effect analogous to the collisions in an ideal gas.[69,70]
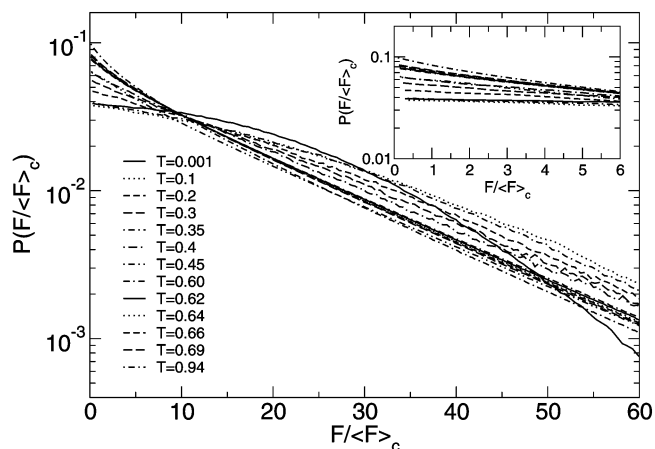
To further compare $P(F)$ with that in granular materials, we calculate the force distribution function scaled with the average force $\langle F \rangle_c$ for a particular configuration, $P(F/\langle F \rangle_c)$. The *T* dependence of $P(F/\langle F \rangle_c)$ vs $F/\langle F \rangle_c$ is shown in Figure 3. We include $P(F/\langle F \rangle_c)$ for several temperatures below $T_0 = 0.48$ for comparison with the force distribution found in ref 1 below T_g. As in Figure 2, the probability of observing forces substantially larger than $\langle F \rangle$ decays exponentially, and the curvature around $\langle F \rangle$ decreases as *T* decreases (see Figure 3 caption). We note that there is a systematic turning of the low-force region in $P(F)$ as well as a change in the curvature of $P(F)$ as the temperature is decreased further. $P(F)$ becomes flat at $T = 0.001$ in the low-force region (see inset of Figure 3), and the curvature of $P(F)$ for $0 < F/\langle F_c \rangle < 6$ does not change as *T* decreases. The change in the curvature of $P(F)$ appears at temperatures significantly lower than T_0 and not in the vicinity of the glass transition. The resemblance of Figures 2 and 3 to similar figures in ref 1 again shows there is no significant distinction between averaging pair forces within a configuration and globally (across configurations), confirming that large force fluctuations, like those found in ref 66 for an out-of-equilibrium system, are not present here.

We note that the reason for using two methods for the calculation of $P(F)$ is the fact that glass-forming liquids, such as our model, are not in equilibrium on all time scales. Long-lived clusters of immobile particles have been reported to persist for times that are orders of magnitude longer that the structural relaxation time τ_α.[71] It is intuitive that if those clusters exist for a long time, forces between mobile particles could have large fluctuations to initiate structural relaxation. Therefore, it is possible that large force fluctuations will be present in super-cooled liquids even after τ_α. If this was the case, then one could observe non-self-averaging of $P(F)$. We demonstrate that this is not the case for our system by comparing two different methods of calculating $P(F)$.

In the experiments and simulations of granular materials and foams, it has been suggested that a signature of jamming is the development of a small peak or plateau around the average force. O'Hern et al. suggested that $P(F)$ will develop a peak if the first peak of $g(r)$ is "sufficiently high and narrow",[72] which they associate with solidlike behavior of the system and a possible signature of the glass transition. Indeed, we observe the sharpening of the first peak in $g(r)$ (not shown here; see, e.g., ref 73) in our system as *T* decreases, but the peak in $P(F)$ is
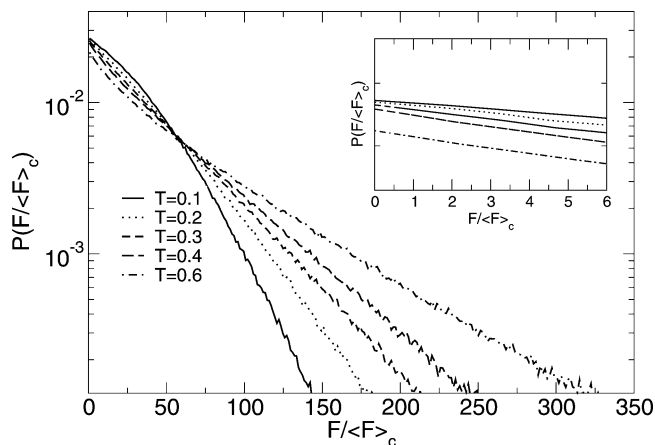
Heterogeneity and Jamming in Glass-Forming Liquids

J. Phys. Chem. B, Vol. 108, No. 51, 2004 **19627**

Figure 4. T dependence of the force distribution $P(F/\langle F \rangle_c)$ vs $F/\langle F \rangle_c$ at several state points in the *NPT* ensemble at $P = 0$. The inset shows a close-up of $P(F)/\langle F \rangle_c$ for forces near $\langle F \rangle_c$.

absent for $T < T_0$ despite the system being solid at those low temperatures. Recall that the jamming transition in granular materials is equivalent to the macroscopic structural arrest of the system. This would correspond to a glass transition in supercooled liquids. Thus for $T > T_0$, we would not expect to observe the peak or plateau in $P(F/\langle F \rangle_c)$ (see Figure 3), and this agrees with our observations. To investigate the behavior of $P(F/\langle F \rangle_c)$ in the glass, we calculate $P(F/\langle F \rangle_c)$ at several T below T_0. These state points are obtained by quenching a configuration previously equilibrated at high temperature, in our case $T = 10.0$, to a desired $T < T_0$, at a nonzero pressure. We do observe that the curvature of $P(F/\langle F \rangle_c)$ around $\langle F \rangle$ decreases as T decreases, and that the slope of log $P(F/\langle F \rangle_c)$ for $10 < \langle F \rangle$ < 60 changes significantly for $T = 0.001$. We observe that a peak is absent in our system at all T, and that a plateau develops only at much lower temperatures ($T = 0.1$) compared to T_0. This demonstrates that development of a peak or plateau is not a necessary condition for a glass transition or a transition to solidlike behavior in dense glass-forming systems.

In the simulations of ref 1, a barostat was used to maintain an average zero pressure. To test if the peak development in $P(F/\langle F \rangle_c)$ depends on the value of the pressure or on choice of thermodynamic ensemble, we performed simulations of our $3D$ binary LJ system at several temperatures in the *NPT* ensemble at zero pressure and calculated the corresponding $P(F/\langle F \rangle_c)$. Figure 4 shows the T dependence of $P(F/\langle F \rangle_c)$ for several *NPT* state points. The pressure is kept at zero for all temperatures. We again observe a change in the curvature in $P(F)$, but only at very low temperatures below T_0, consistent with our findings for the *NVE* system. This again shows that a peak in $P(F/\langle F \rangle_c)$ is not necessary for solidlike behavior of our system. Similar findings have been reported by Reichman and Sastry for another model supercooled liquid.[74]

It is interesting to note that both the *NVE* and *NPT* force distributions $P(F/\langle F \rangle_c)$ have a value of $F/\langle F \rangle_c$ where the distributions cross for almost all T, indicating an isosbestic point. This value is at approximately $F/\langle F \rangle_c = 10$ and 55 for the *NVE* and *NPT* systems, respectively. The reason for such behavior is not immediately obvious and will be investigated in future work. Also note that we tested the self-averaging of $P(F/\langle F \rangle_c)$ for all state points for which the system is a glass. We find no evidence for non-self-averaging of $P(F/\langle F \rangle_c)$ even at those points.

Despite the fact that the peak or plateau in $P(F)$ is observed in many granular materials and some supercooled liquids below

T_g, an open question is its connection to the development of the yield stress in those materials. Several speculations have been made in refs 1 and 72 to explain the jamming scenario and its possible connection to the glass transition. They theorize that "systems jam when there are enough particles in a force chain network to support stress over the time scale of the measurement" which would imply that force chains observed in granular packing may also be important to the glass transition. We test this conjecture in the next section.

V. Generalized Force Chains in Supercooled Liquids

We now investigate the spatial correlations among the instantaneous pairwise forces. Spatially correlated forces can be viewed as networked "paths" of highest, average, or lowest forces in the system. Highest force paths would correspond to the force chains in granular materials, and we refer to them as force chains.

According to ref 75, a force chain in a granular material is a "linear string of rigid particles in point contact". A force chain in a granular material can support a load along its axis. Because we do not apply a load or stress to our system, if such structures exist, they would be induced by lowering the temperature. Inspired by the work of Makse et al.,[76] who studied force chains in a hard sphere system under axial compression, we search the "paths" formed by instantaneous positive forces. In ref 76, the authors found force chains by starting from a sphere at the top of the box of simulated spherical grains and following the path of maximum contact force at every grain. They observed a force-bearing network that was concentrated in a few percolating chains.

In our case, we define force chains such that, for each particle, we find the two neighboring particles that exert the highest force on that particle. This set of three particles constitutes what we call a "trivial chain", because it is always formed by construction. These trivial chains are schematically shown in Figure 5. Longer chains are formed from trivial chains that share two members (Figure 6). A force chain is terminated at any particle included in the chain that has only one "highest force neighbor", as described above. Later, chains that are defined using low and average forces are also calculated in a similar manner as chains defined using the highest forces.

Force chains from the highest instantaneous positive forces would correspond to force chains of point contacts in granular materials. We investigate low and average force chains for the sake of completeness and the fact that we do not have a theory that would *a priori* suggest whether jamming occurs because of high forces or, e.g., average forces. Figure 7 shows a chain of highest forces containing 26 particles in a single configuration at $T = 0.60$. Figure 8 shows all highest force chains at $T = 0.60$ at one snapshot. We refer to chain mass n as the number of particles in that chain. N_{chains} represents the number of nontrivial chains for a particular configuration.

The first trend we investigate is the T dependence of the average mass $\langle n \rangle$ of the force chains and the average number of nontrivial chains $\langle N_{chains} \rangle$. These quantities are shown in Figure 9. The quantities $\langle n \rangle$ and $\langle N_{chains} \rangle$ are averages over the same configurations we used to calculate the force distribution functions, $P(F)$, in section 4. It is evident from Figure 9 that $\langle n \rangle$ and $\langle N_{chains} \rangle$ have at most a very weak temperature dependence. We observe that chains with high forces are on average slightly longer than chains with average forces. We also observe that the average number of chains calculated for the average force subsets is slightly larger than the average number of chains calculated for low and high forces.
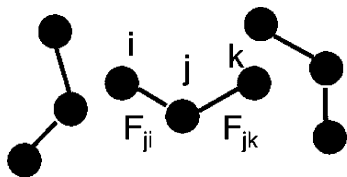
Figure 5. Schematic picture of trivial force chains. Each particle is connected to two neighbors with which it interacts with the highest forces. F_{ji} and F_{jk} are the largest forces on particle j. A similar picture can be drawn for interactions with low or "close to average" forces.
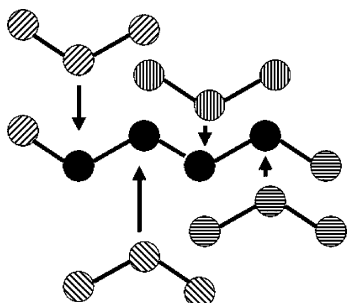

Figure 6. Schematic picture of formation of nontrivial chains. This is an example of a chain of mass six. In this example four trivial chains combine to form a chain of mass six.
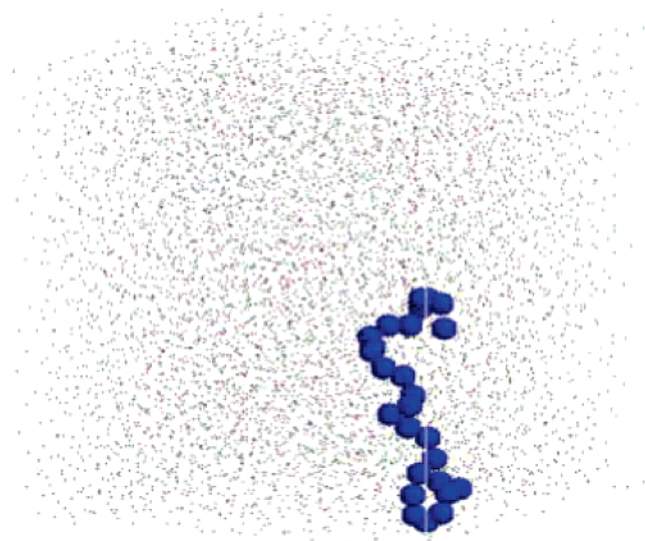

Figure 7. 26-particle chain at $T = 0.60$. The particles in the chain are shown with radius 0.5σ. This is the longest chain for this particular snapshot. This chain does not span the box. Dots represent the rest of the 8000 particles in the system.

To look for any spanning chains (similar to ref 76), we calculate the radius of gyration and end-to-end distance of the force chains, common quantities used to describe the size and shape of polymers.[77] We find that these quantities are also largely independent of temperature (not shown). Therefore, the geometry of these force chains does not change significantly with T. We also do not find any spanning chains that would correspond to the case where the end-to-end distance is equal to the size of the box or where the radius of gyration equals half of the box size. We also investigated the force chain properties in systems out of equilibrium at temperatures below T_{MCT} (e.g., $T = 0.1$), and we do not find a significant difference in chain length or radius of gyration (not shown).

To better understand the difference between chains that are defined using different subsets of forces, we investigate the
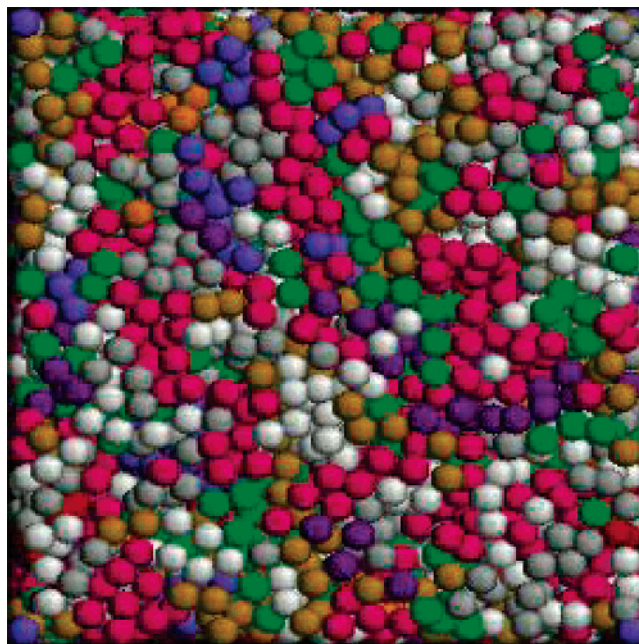

Figure 8. Snapshot of all force chains at $T = 0.60$, obtained from particles experiencing the highest forces. Different colors correspond to force chains with different masses, where mass is defined as the number of particles in the chain. Green indicates the longest chains, and purple indicates the smallest chains. The spatial distribution of force chains with mass n appears to be largely uncorrelated.
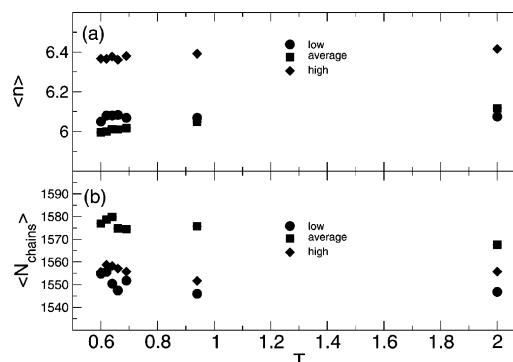

Figure 9. T dependence of the (a) average mass n of the force chains and (b) average number $\langle N_{chains} \rangle$ of nontrivial force chains for low, average, and high pair forces. The error bars are smaller than the symbol size.
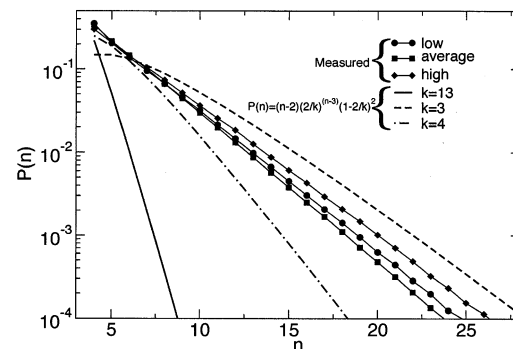

Figure 10. Comparison of the measured mass distributions of force chains for low, average, and high force at $T = 0.60$ and theoretical predictions for different nearest neighbor parameter, k, values.

distribution function of chain mass $P(n)$ for chains defined using low, average, and high forces. $P(n)$ is the probability of finding chains of mass n using the given subset of forces. $P(n)$ is calculated as a normalized histogram of chain masses for each
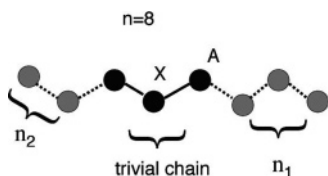
Heterogeneity and Jamming in Glass-Forming Liquids

J. Phys. Chem. B, Vol. 108, No. 51, 2004 **19629**

Figure 11. Example of chain length prediction.

configuration and averaged over all configurations. Figure 10 shows $P(n)$ vs n for chains defined for each subset. We see from $P(n)$ that chains of high forces are, on average, longer than chains of average and low forces, as seen in Figure 9a. Shorter chains defined using average forces may be the consequence of more branching of these chains compared to the chains composed of the highest and lowest forces, which is consistent with the fact that the number of force chains for the average forces is the largest.

To give a theoretical prediction of $P(n)$ for comparison, consider the case where the forces between particles are randomly assigned. Assume that there are k nearest neighbors for a single particle X. If a particle, X, shares one of its highest pair forces with a neighboring particle, A, the probability that the interaction between A and X is one of A's two highest pairwise forces can be approximated as $(2/k)$. Assuming that the chain continues to grow away from its origin and the likelihood of it looping back on itself is small, the probability of adding n_1 additional members on one end of a trivial chain ($n = 3$) (Figure 11) is

$$P(n_1) = \left(\frac{2}{k}\right)^{n_1}\left(1 - \frac{2}{k}\right) \qquad (5)$$

Because there are two ends to the chain and the trivial chain always has three members, the probability for a total chain length $n = n_1 + n_2 + 3$ is

$$P(n) = (n - 2)\left(\frac{2}{k}\right)^{n-3}\left(1 - \frac{2}{k}\right)^2 \qquad (6)$$

where the linear factor $n - 2$ accounts for all combinations of n_1 and n_2 that sum to $n - 3$.

Figure 10 shows predictions of $P(n)$ for various values of the nearest neighbor number parameter, k. From the integration of $g(r)$, the actual number of neighbors in the first neighbor shell is approximately 13. As seen from the figure, the measured

$P(n)$ decays much more slowly than the prediction for entirely randomly assigned forces. Instead, the observations are well bounded by k values of three and four. This gives some measure of the variability in the local force distribution. In other words, the more the local environment of one particle varies from that of its neighbor, the larger the value of k that is found. We also note the possible connection between the force chains found here and the idea of rigidity percolation by Phillips[78] and Thorpe.[79] In rigidity percolation, the mean coordination number $m = 2.4$ represents a threshold below which a network glass is easily deformed. The fact that our nearest neighbor parameter k is close to 3 suggests the possibility that the network of bonds in network glasses and the network of force chains in the LJ mixture studied here share similar properties, and one could use ideas developed in rigidity percolation theory to study force chains in supercooled, non-network-forming liquids.

Figure 12 shows the T dependence of $P(n)$ for chains in low, average, and high force subsets. We find that $P(n)$ can be generally fitted well by a functional form $P(n) = a_1 \exp[-a_2 n]$, where a_1 and a_2 are fitting parameters. We note that the observed exponential behavior of $P(n)$ is analogous to that reported for equilibrium polymerizations[80] of linear polymer chains, in which the bonds between monomers break and recombine at random points along the backbone of the chain. This picture is presumably what happens to the force chain network in our system. Furthermore, the size distribution of strings of cooperative rearranging particles is exponential in all studies of strings performed thus far.[2,3,81] In the case of chains defined using average forces we note a slight T dependence of $P(n)$. It appears that these chains are shorter at lower temperatures, but the distribution is still exponential. In the case of the chains defined using the smallest forces, chains with mass $n = 4$ and $n = 5$ do not fit well with the exponential function (note the slight bend in the curve in Figure 12a).

We conclude this section by noting that the force chains, as constructed, are highly susceptible to thermal fluctuations. More subtle trends may be detectable by using methods to minimize these fluctuations such as quenching to the inherent structure or time averaging over time scales similar to τ_α so as to filter out frequencies higher than those that act over the periods of structural rearrangement. Indeed, we do not find a strong T dependence of the chains defined above. This is surprising because if the highest forces (or any force chains) are related
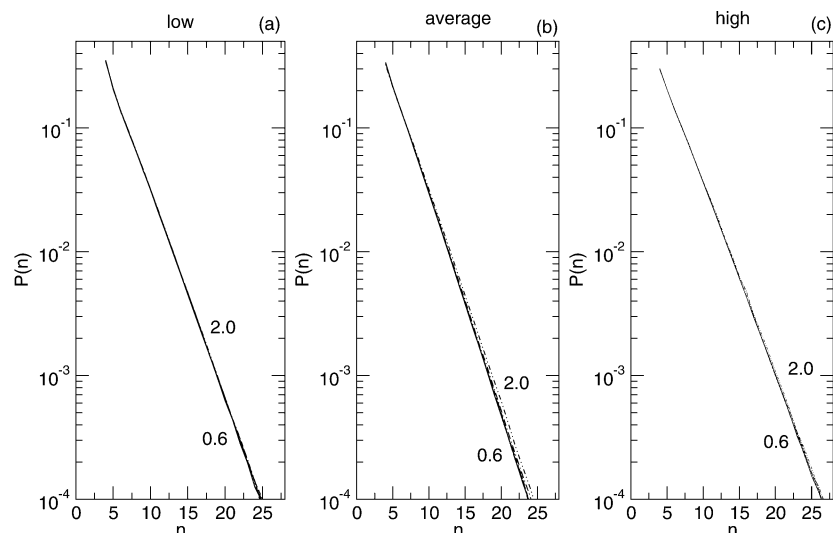

Figure 12. T dependence of the chain mass distribution $P(n)$ for the (a) low, (b) average, and (c) high force. Force chains defined using the average force subset show a slight T dependence.
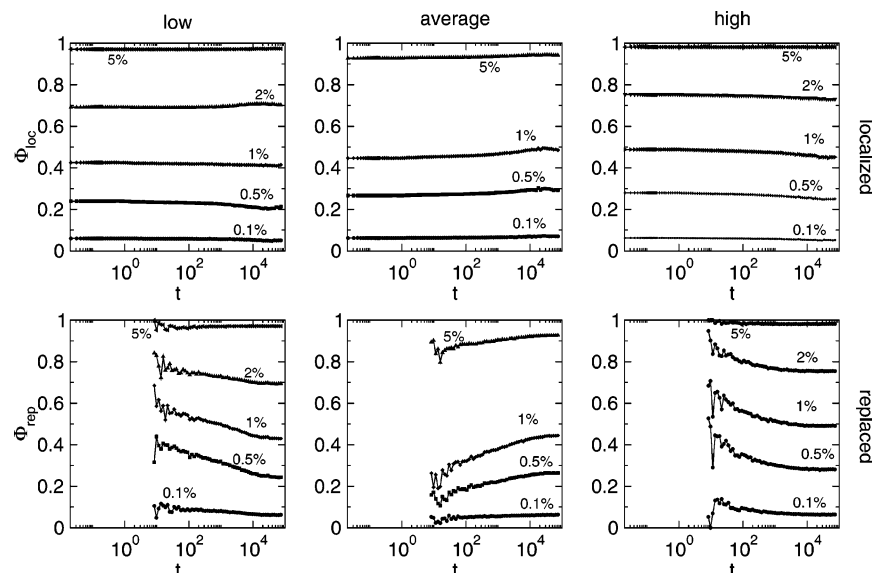
Figure 13. Time dependence of Φ_{loc} (upper three panels) and Φ_{rep} (lower three panels) in the subsets of low, average, and high pair forces at $T = 0.60$. Φ_{rep} is shown for times when Q_D becomes nonzero. Labels on the y axes for average and high forces are the same as for the low forces.

to slowing down of dynamics in supercooled liquids, one might expect to see a temperature dependence in the chain properties. Again, this motivates the study of time-averaged forces in future work.

Because force chains do not couple strongly to density fluctuations they may be linked to local dynamical heterogeneities near T_g. We seek to find a link between SHD and particles that belong to the different regions of the force distribution function, namely, the particle pairs that interact with forces that belong to the exponential tail and average force in the force distribution function, and between SHD and particles in force chains. This is the focus of sections 6 and 7, respectively.

VI. Subsets of Instantaneous Forces

In ref 53, we established a criterion to find localized and replaced particles that we use here to test the relationship between particle mobility and instantaneous pair forces. In section 7, we test the relationship between particle mobilities and force chains. A brief description of how to identify localized, replaced, and delocalized particles can be found in section 3. For every two configurations (one at $t = 0$ and the other at t) we find the number of localized ($Q_S(t)$) and replaced ($Q_D(t)$) particles and calculate all instantaneous pair forces in the configuration at time t. We sort all instantaneous pair forces according to their values and find subsets of particles that interact with pair forces that fall within certain percentages (e.g., 5%, ..., 0.1%) of the lowest, average, and highest pair forces within a given configuration. The considered percentages of these forces are indicated in Figure 13. Because the low, average and high force values change from configuration to configuration, the best indication of typical values for any given configuration may be obtained from examination of Figure 1 (average force) and Figure 2 (high and low forces).

We define a fraction, Φ_{loc} (Φ_{rep}), as the ratio of the number of localized (replaced) particles that are associated with the given subset of pair forces to the total number of localized (replaced) particles, Q_S (Q_D). Φ_{loc} and Φ_{rep} thus relate mobility and

instantaneous forces. Figure 13 shows the time dependence of Φ_{loc} and Φ_{rep} in the given subsets of pair forces at $T = 0.60$.

For the limiting case where all localized and replaced particles belong to the given subset of pair forces, $\Phi_{loc} \equiv 1$ and $\Phi_{rep} \equiv 1$. This is true for subsets larger than $\approx 5\%$ of the pair forces. These fractions are large enough to include nearly all of the system's particles because there are many more pair forces ($\approx 225\,000$) than particles (8000). For lower percentages of the highest pair forces, Φ_{loc} decreases in time from the value expected for the bulk (at $t = 0$ when all particles are localized and Φ_{loc} is simply the probability of finding any particle in the given percentage of pair forces). This suggests that particles that have been localized for long times are less likely to experience high relative forces, if the reason for their long localization is due to being at a local energy minimum. Φ_{rep} decreases in time toward the bulk value (at later times), but this decrease starts on much shorter time scales than Φ_{loc}, possibly because particles that have been replaced (mobile particles) experience higher relative forces at times when they escape from their cages. In the case of low pair forces, the results for Φ_{loc} and Φ_{rep} should be taken with caution because there are two ranges of distance at which particles can experience the lowest force (the tail and well of the potential). The ambiguity in low forces is seen in the inconsistent behavior of Φ_{loc} and Φ_{rep}. This may mask any clear interpretation of the meaning of Φ_{loc} and Φ_{rep} for the lowest forces. In the case of average pair forces, the results are reversed from those of the high pair forces. This means that a larger fraction of localized particles tends to experience average forces at later times, and replaced particles tend to approach the bulk value of the average force.

We note that it is not intuitive that the least mobile particles experience some of the lowest interparticle forces, because the mechanical stability of a particle depends on the vectorial sum of the interparticle forces, and not on extrema or averages of their magnitude. As an example, in granular materials the least mobile particles are those in the force chains that experience the highest forces. Correlations between particle mobility and force chains in our system are investigated in the following section.
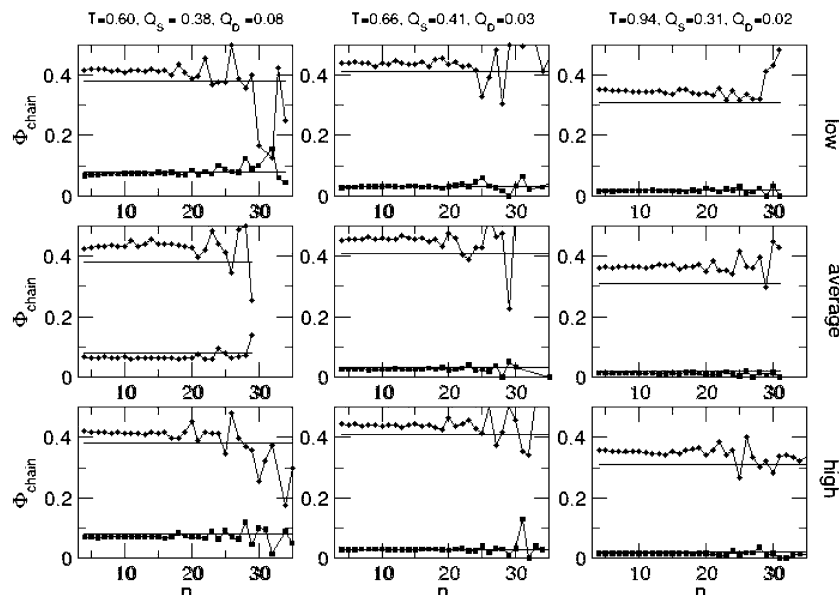
Heterogeneity and Jamming in Glass-Forming Liquids

J. Phys. Chem. B, Vol. 108, No. 51, 2004 **19631**

Figure 14. Fraction, Φ_{chain}, of localized and replaced particles for low, average, and high force chains. The fraction of localized and replaced particles at t_4^{max} is marked with the corresponding T, and it is indicated by the solid lines on each panel.

VII. Fraction of Localized and Replaced Particles in Force Chains

To look for a connection between force chains defined via instantaneous positive pairwise forces and mobility, we calculate the fraction of localized and replaced particles in each chain for all subsets of forces for which force chains are defined. This fraction is calculated in the following manner. For each configuration at t, we identify the force chains and localized and replaced particles with respect to an initial configuration at $t = 0$, and for each chain of mass n in the configuration at t we count the number of localized and replaced particles and divide by n. After this, we average those fractions over all equally spaced configurations. Figure 14 shows the fraction of localized and replaced particles in the chains of high, average, and low force at t_4^{max} (defined for each T in ref 53, and section 3) at $T = 0.60$, $T = 0.66$, and $T = 0.94$. We examine the configurations at the particular time t_4^{max} because, as explained in section 3, SHD as measured by $\chi_4(t)$ and the correlation length $\xi_4(t)$ is most pronounced then. If SHD in supercooled liquids and granular materials share common mechanisms, one might expect the effects of jamming to be most detectable at this time. The fraction of localized and replaced particles is shown in Figure 14 for each T. The first column in Figure 14 represents Φ_{chain} at $T = 0.60$ for low, average, and high force chains. The second and third column contain data for Φ_{chain} at $T = 0.66$ and $T = 0.94$, respectively.

From Figure 14 we see that Φ_{chain} is essentially constant for $n \leq 20$ for both localized and replaced particles. For chain masses greater than 20, Φ_{chain} becomes noisy because of poor statistics. For chains with $n \leq 20$, Φ_{chain} has values slightly higher than the fraction of localized particles in the bulk, Q_S (Q_S is indicated by solid lines in Figure 14). This means that localized particles are more likely to be found in chains with intermediate mass than would be expected from the fraction of localized particles (Q_S) in the system. Φ_{chain} has values equal to or slightly lower than the fraction of replaced particles in the bulk (Q_D is also indicated by solid lines in Figure 14). This means that replaced particles are equally or less likely to be found in the chains of intermediate mass based on their bulk population. These behaviors are basically universal regardless

of the subset of forces in which the force chains are defined. Therefore, we cannot make a simple connection with mobility, and force chains as defined here probably do not play the same role as those found in granular materials.

The population of localized and replaced particles in the force chains can be explained if we suppose that localized particles reside in a local environment that is less susceptible to force perturbations than delocalized particles. Imagine an "intrinsic" high force chain that would be associated with the inherent structure and introduce a perturbation near the chain that propagates perpendicular to it. This perturbation can temporarily change which neighbors of a given particle in the chain interact with it via the highest relative force, thereby breaking the chain. Such perturbations are the manifestation of temperature in the system. Because the localized particles are more likely to be found in nontrivial chains, one might speculate that something about their local environment makes them resistant to these perturbations at least with respect to the relative forces exerted by their neighbors.

VIII. Discussion

In this paper we examined the relationship between jamming in granular materials and SHD in supercooled liquids. We focused on the instantaneous, positive forces between neighboring particles in a model glass-forming liquid (in analogy with normal or contact forces between grains in granular materials), and calculated the force distribution function $P(F)$. We did not find a peak in this quantity at any T whether above or below T_g, in contrast to the model supercooled liquids studied in ref 1. We also found a possible connection between instantaneous force magnitude and long term mobility. We defined force chains in our model glass-forming liquid, and on the basis of our results from section 5, we found force chains much longer than those that might be expected for randomly assigned forces. These force chains probably do not play the same role in this supercooled liquid as in granular materials because they do not show a strong temperature dependence.

Force chains may, however, indicate a difference in the evolution of the local environment of particles with different mobilities which may be connected with cooperative and

stringlike motion found in model supercooled liquids close to T_g. Microscopic details of local particles dynamics and the mechanism by which particles move along stringlike paths is studied in ref 3 in a glass-forming Dzugotov liquid. The authors show that simultaneous motion of individual particles along the string depends on the length of the string, and that for shorter strings the motion is highly coherent and for longer strings motion is coherent only within short segments containing as many as seven particles (microstrings). We note the similarity between the anatomy of strings and force chains studied here by comparing a snapshot of a string in Figure 10 of ref 3 and Figure 7 of this paper (remember that the criterion for a string is completely different from the criterion for a force chain). We also note that both the distribution of mass of force chains and distribution of string length appear to be exponential. Although the mass of the force chains does not grow as a function of T, in contrast to string length, these distributions are, to our knowledge, the only two distributions of quantities associated with force and particle mobility measured in supercooled liquids that obey exponential laws. This leads us to pose certain questions: What is the relationship between force chains and strings? Is it possible that force chain networks provide a characteristic structural path along which strings may occur? Could frequent defects in the force chain network due to breakage and recombination of trivial force chains be associated with the local liquid excitations proposed by Garrahan and Chandler[56] and provide a path for stringlike motion? Answers to those questions may help us to understand the origin of SHD in glass-forming liquids. Further work on the relationship between strings and force chains is ongoing.

References and Notes

(1) O'Hern, C. S.; Langer, S. A.; Liu, A. J.; et al. *Phys. Rev. Lett.* **2001**, *86*, 111.

(2) Donati, C.; Douglas, J. F.; Kob, W.; Poole, P. H.; Plimpton, S. J.; Glotzer, S. C. *Phys. Rev. Lett.* **1998**, *80*, 2338.

(3) Gebremichael, Y.; Vogel, M.; Glotzer, S. C. *J. Chem. Phys.* **2004**, *120*, 4415.

(4) Rottler, J.; Robbins, M. O. *Phys. Rev. Lett.* **2002**, *89*, 195501.

(5) Trappe, V.; Prasad, V.; Cipelletti, L.; et al. *Nature* **2001**, *411*, 772.

(6) Durian, D. J. *Phys. Rev. Lett.* **1995**, *75*, 4780.

(7) de Gennes, P. G. *Rev. Mod. Phys.* **1999**, *71*, S374.

(8) Kadanoff, L. P. *Rev. Mod. Phys.* **1999**, *71*, 435.

(9) Jaeger, H. M.; Nagel, S. R.; Behringer, R. P. *Rev. Mod. Phys.* **1996**, *68*, 1259.

(10) Nowak, E. R.; Knight, J. B.; Ben-Naim, E.; et al. *Phys. Rev. E* **1998**, *57*, 1971.

(11) Knight, J. B.; Fandrich, C. G.; Lau, C. N.; et al. *Phys. Rev. E* **1995**, *51*, 3957.

(12) D'Anna, G.; Gremaud, G. *Phys. Rev. Lett.* **2001**, *87*, 254302.

(13) Liu, A. J.; Nagel, S. R. *Nature* **1998**, *396*, 21. Liu, A. J., Nagel, S. R., Eds. *Jamming and rheology: constrained dynamics on microscopic and macroscopic scales*; Taylor and Francis: London, New York, 2001.

(14) Longhi, E.; Easwar, N.; Menon, N. *Phys. Rev. Lett.* **2002**, *89*, 045501.

(15) Howell, D.; Behringer, R. P.; Veje, C. *Phys. Rev. Lett.* **1999**, *82*, 5241.

(16) Roux, J. N. *Phys. Rev. E* **2000**, *61*, 6802.

(17) Radjai, F.; Jean, M.; Moreau, J. J.; et al. *Phys. Rev. Lett.* **1996**, *77*, 274.

(18) Tkachenko, A. V.; Witten, T. A. *Phys. Rev. E* **1999**, *60*, 687.

(19) Farr, R. S.; Melrose, J. R.; Ball, R. C. *Phys. Rev. E* **1997**, *55*, 7203.

(20) Kustanovich, T.; Rabin, Y.; Olami, Z. *Phys. Rev. B* **2003**, *67*, 104206.

(21) Bohmer, R.; Chamberlin, R. V.; Diezemann, G.; et al. *J. Non-Cryst. Solids* **1998**, *235*, 1.

(22) Doliwa, B.; Heuer, A. *Phys. Rev. Lett.* **1998**, *80*, 4915.

(23) Yamamoto, R.; Onuki, A. *Phys. Rev. Lett.* **1998**, *81*, 4915. Onuki, A.; Yamamoto, Y. *J. Non-Cryst. Solids* **1998**, *235–237*, 34. Onuki, A.; Yamamoto, Y. *Inter. J. Mod. Phys. C* **1553**, *10*, 1999.

(24) Perera, D.; Harrowell, P. *J. Non-Cryst. Solids* **1998**, *235–237*, 314. Perera, D.; Harrowell, P. *Phys. Rev. E* **1999**, *59*, 5721. Perera, D.; Harrowell, P. *Phys. Rev. E* **1652**, *54*, 1996. Fynewever, H.; Harrowell, P. *J. Phys.: Condens. Matter* **2000**, *12*, 6305.

(25) Mel'cuk, A. I.; Ramos, R. A.; Gould, H.; Klein, W.; Mountain, R. D. **1995**, *75*, 2522. Johnson, G.; Mel'cuk, A. I.; Gould, H.; Klein, W.; Mountain, R. D. *Phys. Rev. E* **1998**, *57*, 5707.

(26) Muranaka, T.; Hiwatari, Y. *Phys. Rev. E* **1995**, *51*, R2735. Hiwatari, Y.; Muranaka, T. *J. Non-Cryst. Solids* **1998**, *235–237*, 19.

(27) Dzugutov, M.; Simdyankin, S. I.; Zetterling, F. H. M. *Phys. Rev. Lett.* **2002**, *89*, 195701.

(28) Kob, W.; Donati, C.; Poole, P. H.; Plimpton, S. J.; Glotzer, S. C. *Phys. Rev. Lett.* **1997**, *79*, 2827.

(29) Schmidt-Rohr, K.; Spiess, H. W. *Phys. Rev. Lett.* **1991**, *66*, 3020.

(30) Chang, I.; Sillescu, H. *J. Phys. Chem. B* **1997**, *101*, 8794.

(31) Böhmer, R.; et al. *J. Non-Cryst. Solids* **1998**, *235–237*, 1.

(32) Cicerone, M. T.; Blackburn, F. R.; Ediger, M. D. *Macromolecules* **1995**, *28*, 8224. Cicerone, M. T.; Ediger, M. D. *J. Chem. Phys.* **1996**, *104*, 7210. Blackburn, F. R.; et al. *J. Non-Cryst. Solids* **1994**, *172–174*, 256. Swallen, S. F.; Bonvallet, P. A.; McMahon, R. J.; Ediger, M. D. *Phys. Rev. Lett.* **2003**, *90*, 015901.

(33) Hall, D. B.; Dhinojwala, A.; Torkelson, J. M. *Phys. Rev. Lett.* **1997**, *79*, 103.

(34) Heuer, A.; et al. *Phys. Rev. Lett.* **1995**, *95*, 2851;

(35) Andreozzi, L.; Di Schino, A.; Giordano, M.; Leporini, D. *Europhys. Lett.* **1997**, *38*, 669.

(36) Richert, R. *Chem. Phys. Lett.* **1992**, *199*, 355. Richert, R.; Stickel, F.; Fee, R. S.; Maroncelli, M. *Chem. Phys. Lett.* **1994**, *229*, 302. Wendt, H.; Richert, R. *Phys. Rev. E* **2000**, *61*, 1722. Yang, M.; Richert, R. *J. Chem. Phys.* **2001**, *115*, 2676. Richert, R. *J. Non-Cryst. Solids* **1994**, *172–174*, 209.

(37) Russell, E. V.; Israeloff, N. E. *Nature* **2000**, *408*, 695.

(38) Schiener, B.; Böhmer, R.; Loidl, A.; Chamberlin, R. V. *Science* **1996**, *274*, 752. Schiener, B.; Chamberlin, R. V.; Diezemann, G.; Böhmer, R. *J. Chem. Phys.* **1997**, *107*, 7746.

(39) Russina, M.; Mezei, F.; Lechner, R.; Longeville, S.; Urban, B. *Phys. Rev. Lett.* **2000**, *84*, 3630.

(40) Weeks, E.; Crocker, J. C.; Levitt, A. C.; Schofield, A.; Weitz, D. A.; *Science* **2000**, *287*, 627. Weeks, E. R.; Weitz, D. A. *Phys. Rev. Lett.* **2002**, *89*, 095704.

(41) Kegel, W. K.; van Blaaderen, A. *Science* **2000**, *287*, 290.

(42) van Blaaderen, A.; Wiltzius, P. *Science* **1995**, *270*, 1177.

(43) Deschenes, L. A.; Vanden Bout, D. A. *Scinece* **2001**, *292*, 255.

(44) Marcus, A. H.; Schofield, J.; Rice, S. A. *Phys. Rev. E* **1999**, *60*, 5727; **2000**, *61*, 7260.

(45) Sillescu, H. *J. Non-Cryst. Solids* **1999**, *243*, 81 and references therein.

(46) Ediger, M. D. *Annu. Rev. Phys. Chem.* **2000**, *51*, 99.

(47) Richert, R. *J. Condens. Matter* **2002**, *14*, R703.

(48) Bennemann, C.; Donati, C.; Baschnagel, J.; Glotzer, S. C. *Nature* **1999**, *399*, 246.

(49) Donati, C.; Glotzer, S. C.; Poole, P. H.; Kob, W.; Plimpton, S. J. *Phys. Rev. E* **1999**, *60*, 3107.

(50) Donati, C.; Poole, P. H.; Glotzer, S. C. *Phys. Rev. Lett.* **1999**, *82*, 6064.

(51) Glotzer, S. C.; Donati, C. *J. Phys.: Condens. Matter* **1999**, *11*, A285.

(52) Glotzer, S. C. *J. Non-Cryst. Solids* **2000**, *274*, 342.

(53) Lačević, N., Starr, F. W.; Schrøder, T. B.; Glotzer, S. C. *J. Chem. Phys.* **2003**, *119*, 7372.

(54) Stillinger, F. H.; Hodgdon, J. *Phys. Rev. E* **1994**, *50*, 2064; **1996**, *53*, 2995. Stillinger, F. H. *J. Chem. Phys.* **1988** *89*, 6461 and references therein.

(55) Vogel, M.; Glotzer, S. C. *Phys. Rev. Lett.* **2004**, *92*, 255901. Vogel, M.; Glotzer, S. C. submitted to *Phys. Rev. E.* Bergroth, M.; Vogel, M.; Glotzer, S. C. Manuscript in preparation.

(56) Garrahan, J. P.; Chandler, D. *Phys. Rev. Lett.* **2002**, *89*, 03570. Garrahan, J. P.; Chandler, D. *Proc. Natl. Acad. Sci. U.S.A.* **2003**, *100*, 9710.

(57) Glotzer, S. C. *Phys. World* **2000**, *13*, 22.

(58) Steve Plimpton, Sandia National Labs, www.cs.sandia.gov/~sjplimp.

Heterogeneity and Jamming in Glass-Forming Liquids

J. Phys. Chem. B, Vol. 108, No. 51, 2004 **19633**

(59) Wahnstrom, G. *Phys. Rev. A* **1991**, *44*, 3752.

(60) Schrøder, T. B. Hopping in Disordered Media: A Model Glass Former and A Hopping Model, cond-mat/0005127.

(61) Glotzer, S. C.; Novikov, V. N.; Schrøder, T. B. *J. Chem. Phys.* **2000**, *112*, 509.

(62) Schrøder, T. B.; Sastry, S.; Dyre, J. C.; et al. *J. Chem. Phys.* **2000**, *112*, 9834.

(63) Schrøder, T. B.; Dyre, J. C. *J. Non-Cryst. Solids* **1998**, *235*, 331.

(64) Lačević, N. Dynamical heterogeneity in simulated glass-forming liquids studied via a four-point spatiotemporal density correlation function. Dissertation, The Johns Hopkins University, 2003.

(65) Novikov, V. N.; Sokolov, A. P. *Phys. Rev. E* **2003**, *67*, 031507.

(66) O'Hern, C. S.; Langer, S. A.; Liu, A. J.; et al. *Phys. Rev. Lett.* **2002**, *88*, 075507.

(67) Tewari, S.; Schiemann, D.; Durian, D. J.; et al. *Phys. Rev. E* **1999**, *60*, 4385.

(68) Langer, S. A.; Liu, A. J. *Europhysics Lett.* **2000**, *49*, 68.

(69) Coppersmith, S. N.; Liu, C.; Majumdar, S.; et al. *Phys. Rev. E* **1996**, *53*, 4673.

(70) Liu, C. H.; Nagel, S. R.; Schecter, D. A.; et al. *Science* **1995**, *269*, 513.

(71) Doliwa, B.; Heuer, A. *J. Non-Cryst. Solids* **2002**, *307*, 32.

(72) O'Hern, C. S.; Silbert, L. E.; Liu, A. J.; et al. *Phys. Rev. E* **2003**, *68*.

(73) Lačević, N.; Starr, F. W.; Schrøder, T. B.; et al. *Phys. Rev. E* **2002**, *66*, 030101.

(74) Private communications.

(75) Cates, M. E.; Wittmer, J. P.; Bouchaud, J. P.; et al. *Phys. Rev. Lett.* **1998**, *81*, 1841.

(76) Makse, H. A.; Johnson, D. L.; Schwartz, L. M. *Phys. Rev. Lett.* **2000**, *84*, 4160.

(77) Doi, M.; Edwards, S. F. *The theory of polymer dynamics*; Oxford University Press: New York 1988.

(78) Phillips, J. C. *J. Non-Cryst. Solids* **1979**, *34*, 153; **1981**, *43*, 37.

(79) Thorpe, M. *J. Non-Cryst. Solids* **1983**, *57*, 355.

(80) Rouault, Y.; Milchev, A. *Phys. Rev. E* **1997**, *55*, 2020. Greer, S. C. *Adv. Chem. Phys.* **1996**, *94*, 261. Bellissent, R.; Descotes, L.; Pfeuty, P. *J. Phys. Condens. Matter* **1994**, *A211*, 6.

(81) Aichele, M.; Gebremichael, Y.; Starr, F. W.; Baschnagel, J.; Glotzer, S. C. *J. Chem. Phys.* **2003**, *119*, 5290.